Marangoni Flow of Ag Nanoparticles from the Fluid−Fluid Interface†

Donald D. Johnson, Jr., Barry Kang, John L. Vigorita, Alec Amram, and Eileen M. Spain*

Department of Chemistry, Occidental College, 1600 Campus Road, Los Angeles, California 90041

Received: March 15, 2008; Revised Manuscript Received: August 11, 2008

Fluid flow is observed when a volume of passivated Ag nanoparticles suspended in chloroform is mixed with a water/ethanol (v/v) mixture containing acidified 11-mercaptoundecanoic acid. Following mechanical agitation, Ag nanoparticles embedded in a film are driven from the organic−aqueous interface. A reddish-brown colored film, verified by transmission electron microscopy to contain uniformly dispersed Ag nanoparticles, is observed to spontaneously climb the interior surface of an ordinary, laboratory glass vial. This phenomenon is recorded by a digital video recorder, and a measurement of the distance traveled by the film front versus time is extracted. Surface (interfacial) tension gradients due to surfactant concentration, temperature, and electrostatic potential across immiscible fluids are known to drive interface motion; this well-known phenomenon is termed Marangoni flow or the Marangoni effect. Experimental results are presented that show the observed mass transfer is dependent on an acid surfactant concentration and on the volume fraction of water in the aqueous phase, consistent with fluid flow induced by interfacial tension gradients. In addition, an effective desorption rate constant for the Marangoni flow is measured in the range of ∼0.01 to ∼1 s^{-1} from a fit to the relative film front distance traveled versus time data. The fit is based on a time-dependent expression for the surface (interface) excess for desorption kinetics. Such flow suggests that purposeful creation of interfacial tension gradients may aid in the transfer of 2- and 3-dimensional assemblies, made with nanostructures at the liquid−liquid interface, to solid surfaces.

Introduction

Free surface flow is an important phenomenon to anticipate, understand, and perhaps apply advantageously.[1−3] Free surface flow takes place on various scales, ranging from tidal wave flow to nanoliter flow.[1] The latter case of 1 nL corresponds to 10^6 μm^3, the scale of intense scrutiny in the field of microfluidics. Microfluidics continues to enjoy participation from a wide range of scientific communities to develop automation of biology and chemistry in a parallel manner, just as microelectronic circuitry transformed computing when circuit dimensions were decreased.[3] To reach this goal, the physics of fluid flow through tiny channels is required. Various types of fluid flow are typically understood by considering competing phenomena.[3] In free surface flow, the competing phenomena of viscous shear and capillary stresses are unbalanced due to interfacial tension gradients. Hence, free surface flows may be of keen interest to some applications in microfluidic settings. However, if practically the utilization of the interfacial tension gradients to coat or move mass prove too cumbersome in microfluidics,[3] then application of this phenomenon to form interesting nanostructure-containing films or coatings on surfaces may be fruitful.

The liquid−liquid interface, which has been successfully utilized to assemble micron-sized particles, is now also considered a useful space to assemble nanoparticles, and nanometer-sized structures in general.[4−17] The alteration of the surface properties of nanoparticles results in their assembly at a variety of liquid−liquid interfaces where the goal is to wet both phases at (or near, depending of nanoparticle surface chemistry) the three-phase contact angle $\theta = 90°$.[4,5,7] In that particular case, the nanoparticles have an equal hemisphere in each phase. Due to the nanometer radius of a nanoparticle, however, the interfacial energy is comparable to thermal energy kT, and thus these assemblies have been categorized, from elegant measurements, as rather dynamic[7] even if slight variations of the three phase contact angle occur. Of interest of late are nanoparticles with charged ligands suspended in aqueous solutions.[9−12] Our group made a contribution to this area of investigation with Ag nanoparticles dissolved in organic solvent, in what is a general method.[13] Also noted in our study,[13] and some earlier studies in other laboratories with charged nanoparticles,[9−11] was the observation of film transfer to the interior glass surface of the vial or container. In 2006, Reincke et al. additionally referenced Sastry[9] as recognizing Marangoni flow as the likely mechanism for film transfer to a glass solid surface. Finally, the many optical properties of nanostructures, particularly those composed of the coinage metals, offer an enticing series of applications,[18,19] particularly if such structures could be incorporated easily into films or coatings. These investigations, taken in sum, and Sastry's inferences in particular about a Marangoni effect, warranted this investigation. In fact, our hope is to invigorate Sastry's insight into Marangoni flow with this work as a means to transfer 2- and 3-dimensional superlattices from fluid−fluid interfaces onto surfaces, particularly with coinage metal nanometer scale components.

Herein we describe a fluid flow with silver nanoparticles (5−8 nm diameter). And, whereas the interfacial region in our experimental system allows nanoparticles to assemble under certain conditions, other conditions permit this interface to flow such that a film with uniformly distributed nanoparticles is spontaneously transferred to a glass surface. Fluid flow results when two nominally immiscible fluids, an organic phase that contains a suspension of passivated Ag nanoparticles and an aqueous phase that contains an alkanoic acid, are mixed. In our previously published work, a film containing Ag nanoparticles

† Part of the "Stephen R. Leone Festschrift".

* Corresponding author. Phone: (323)-259-2940. Voice: (323)-341-4912. E-mail: emspain@oxy.edu.

10.1021/jp802273j CCC: $40.75
Published on Web 09/10/2008

formed at the organic−aqueous interface when an aqueous mixture was placed in contact and mixed with Ag nanoparticles suspended in chloroform.[13] In those experiments, the aqueous phase was composed of a 50/50 or 40/60 (v/v) water/ethanol solution containing acidified 11-mercaptoundecanoic acid. We noted at that time a wicking effect, where the film could be coaxed to leave the interface between the two fluids, and wick the interior glass surface by tilting the vial. In this work, efficacious, spontaneous coating of a glass surface with a film embedded with Ag nanoparticles is reported. It is deduced from qualitative and quantitative measurements that the motion of this film to climbs the interior walls of a glass vial originates from interfacial tension gradients as described by the Marangoni effect.[20,21]

Theoretical Synopsis

The Navier−Stokes equation provides the continuum physics necessary to understand flow of an incompressible, Newtonian fluid.[3,22] The stress tensor in the Navier−Stokes equation most concerns us here, and contains both normal and tangential components. In brief, the balance of viscous and capillary stresses can be expressed with the dimensionless capillary number, *Ca*, as

$$Ca = \eta u/\gamma \tag{1}$$

where u is the scalar velocity, η is the shear viscosity, and γ is the interfacial tension. The resulting scalar velocity of fluid flow, u, is then presented as

$$u \sim \Delta\gamma/\eta \tag{2}$$

where $\Delta\gamma$ is the interfacial tension gradient.[3] The Marangoni stresses are exerted along the interface due to interfacial tension gradients ($\Delta\gamma$), and subsequently set the interface in motion if the viscous stresses (resisting motion) and Marangoni stresses are unbalanced.[3]

The liquid−liquid interfacial tension may be affected by temperature, surfactant concentration, and electrostatic potential. In this synopsis, only surfactant concentration at the interface is related to the interfacial tension gradient. As developed by Abbott et al.,[23] the velocity for this flow can be equated to the time-dependent surface (interface) excess (Γ) and the Gibbs adsorption isotherm, that, in turn, is a function of surface tension. The Gibbs adsorption isotherm[24] is

$$\Gamma = -(c/RT)\mathrm{d}\gamma/\mathrm{d}c \tag{3}$$

where Γ is the interface excess (the solute at the interface) and c is the solute concentration in the bulk, and states that the interfacial tension γ decreases when a solute is enriched at an interface. In addition, if it is presumed that diffusion of the solute in and out the interface from the bulk is much slower than Marangoni flow,[23,24] and if the flow occurs within the reference frame of the Marangoni velocity,[23] then the interface excess function is

$$\mathrm{d}\Gamma(t)/\mathrm{d}t = \text{rate of adsorption} + \text{rate of desorption} \tag{4}$$

and

$$\mathrm{d}\Gamma(t)/\mathrm{d}t = k_{\mathrm{ads}}c_{\mathrm{s}}(1 - \Gamma/\Gamma_{\infty}) - k_{\mathrm{des}}\Gamma \tag{5}$$

where k_{des} is the desorption rate constant, k_{ads} is the adsorption rate constant, and c_{s} is the sublayer surfactant concentration.[23−25] If it is further assumed that the stresses induced by interfacial tension gradients as Ag nanoparticles assemble move the film *away from the fluid−fluid interface*, then desorption is the main factor in the kinetics, as it was with a different kind of system studied by Abbott et al.,[23] such that

$$\mathrm{d}\Gamma(t)/\mathrm{d}t = -k_{\mathrm{des}}\Gamma \tag{6}$$

and

$$\Gamma(t) = \Gamma(0)\exp(-k_{\mathrm{des}}t) \tag{7}$$

We infer that the interface excess rate of change scales as the interfacial tension gradient as

$$\Gamma(t) \sim \Delta\gamma \tag{8}$$

Thus, relating eqs 8, 7, and 2 yields

$$u \sim \exp(-k_{\mathrm{des}}t) \tag{9}$$

and an expression for the film front distance as a function of time, $x(t)$, can be represented as

$$x(t) \sim \exp(-k_{\mathrm{des}}t) \tag{10}$$

where k_{des} is the effective desorption rate constant for the free surface flow due to a surfactant concentration gradient at the interface. For a recent review of Marangoni instabilities and oscillations due to surfactant transport across liquid interfaces, Kovalchuk and Vollhardt provide a rigorous theoretical analysis.[26]

Experimental Methods

Ag Nanoparticle Synthesis. We employed a synthesis that is a slight variant of the one described by Klabunde et al.[27] and used previously by our laboratory to make films embedded with Ag nanoparticles at the liquid−liquid interface.[13] In that study, we inferred that these nanoparticles are passivated with physisorbed TAB (tetraoctylammonium bromide), a common phase transfer reagent in organic synthesis, as well as chemisorbed dodecanethiol. Briefly, 0.9775 g of TAB was added to 5 mL of toluene, previously degassed with N_2 gas for about 2 h, and sonicated until complete dissolution is achieved. Next, 0.0312 g of $AgNO_3$ was added to the toluene and TAB mixture, and sonicated to complete dissolution. With constant stirring, a volume of 15 μL of dodecanethiol was added. Following additional stirring for 18 min, 0.0987 g of $NaBH_4$ dissolved in 3 mL of H_2O was added, followed by 3 h of stirring. The resulting passivated Ag nanoparticles were washed once in ethanol and resuspended in dried chloroform. Measurement of λ_{max} with Ultraviolet−visible (UV−vis) spectrophotometry was routinely used to verify nanoparticle formation and qualitative size distribution of Ag nanoparticles (data not shown). Occasionally, transmission electron microscopy (Phillips EM 430, 300 keV) was employed to characterize size distributions (data not shown), and typically our syntheses yielded nanoparticles with diameters of about 5−8 nm.

Emulsion and Film Formation. The two liquid phases were placed in contact. An aqueous phase was prepared in an ordinary borosilicate vial (dimensions 1.7 cm diameter by 6 cm height). The aqueous phase was composed of a water/ethanol mixture by volume fraction, 10 or 5 mM 11-mercaptoundecanoic acid (MUA), and added HCl(aq) such that the pH was about 1−2, a pH below the pK_{a} of MUA assembled at an interface.[28] To this aqueous phase was added the once-washed, concentrated nanoparticle suspension in dry chloroform in 1:1 or 2:1 aqueous to chloroform volume proportions. Experiments were conducted with concentrated suspensions, to better observe and measure the film transfer with digital images and video, respectively. These suspensions were once-washed to preserve TAB; TAB is required for film formation. Due to its density, the chloroform layer rested below the aqueous phase, so in all experiments the top layer is the aqueous solution. It should be noted that no

film transfer is observed over a 1 h time period when the two fluids were in contact, unless some sort of mechanical agitation occurred. The two phases were vigorously mixed by hand or with magnetic bar stirring, and an emulsion was created, and as described in the Results and Discussion section, a film created. In addition, such mechanical agitation necessarily prewetted the interior glass vial surface. Vials were capped, thus saturated vapors within the vial may play a role.

Characterization of the Film by Transmission Electron Microscopy. The film was characterized by transmission electron microscopy (TEM) with an improved method. In our previous technique,[13] the film was then captured by tilting an opened vial and lifting a TEM grid near the fluid−fluid interface. The grid was dried, and imaged, where nanoparticles and in some cases nanostructures (presumably from annealed nanoparticles) in multilayers were observed. In this work, a portion of the film was pipetted from the emulsion region at the fluid−fluid interface for an experiment with 1:1 aqueous to chloroform by volume proportions with 60/40 (v/v) water/ethanol and 10 mM MUA in the aqueous phase. The contents of the pipet were transferred to the surface of distilled water in a glass Petri dish. Immediately following, though some chloroform was still present, the film was transferred via the Langmuir−Schaefer method to a TEM grid (200 μm, amorphous carbon grids, Ted Pella). Without delay, the grid was placed in the TEM for imaging.

Fluid Flow. As the emulsion phase separated, a reddish brown film spontaneously climbed the interior surface of a capped, ordinary borosilicate glass vial. The film climbed the glass surface *from the top of the aqueous layer*, where some of the emulsion was suspended after mixing; presumably these were the comparatively smaller droplets of the emulsion. This observation is different from what Reincke et al.[11] noted in 2006 with their Au colloidal system, where the climbing film begins at the contact plane of the water/heptane interface. In addition, in some cases, the emulsion *between aqueous and chloroform layers* did not completely phase separate within the time frame of measurements, whereas in other cases it did. However, one qualitative observation was immediately recorded with each trial: the climbing rate decreases with time as the film approaches its equilibrium height.

To test the possibility that surface flow was induced by interfacial tension gradients, two experiments were conducted. In the first case, the MUA concentration was halved, in principle affecting the amount of MUA, a surfactant, at the interface. The second experiment varied the water volume fraction in the water/ethanol mixtures of the aqueous phase. Here, we expected that greater fractions of water would create a larger interfacial tension overall at the fluid−fluid interface, affecting the amount of mass transfer. Finally, to ensure that the phase separation of the emulsion *between the two fluids* did not dramatically affect the $x(t)$ versus time measurements from the top of the aqueous phase, the experiments were repeated with one change: the chloroform volume was halved.

Using a digital video recorder, the distance traveled by the film was measured in centimeters using a metric ruler mounted vertically and adjacent to the vial. Measurements began when a climbing, contiguous film could be confidently identified. Like Abbott et al.,[23] we faced the challenge of collecting early time data. The earliest distance measurements ($t = 0.00$ s) recorded throughout our investigation, and in all the quantitative data presented in this paper, were measured within 0.2 cm above the top of the aqueous layer. The estimated errors in the relative film front distance and time are ± 0.07 cm and ± 0.1 s, respectively. Distance that the film front traveled was an average of the highest and lowest distances of the film front at a given time. The film front distance plotted was relative to the starting distance for each measurement.

Results and Discussion

Following our 2005 study, it was noticed that if the water volume fraction in the aqueous phase is increased relative to the ethanol fraction, a mass transfer from the fluid−fluid interface to the interior surface of a borosilicate glass vial occurs with increasing rate.[29] Thus, we realized that we could control the transfer efficacy of the nanoparticle film to glass. Ultimately, that observation coupled with prior studies in the literature[9,11,23] led us to the hypothesis that this flow was set in motion according to the Marangoni effect, and that the rate of transfer is consistent with the time-dependent nature of surfactant concentration at the fluid−fluid interface.

Emulsion Formation Is Required. Mixing of the two nominally immiscible phases is required to observe this phenomenon. Unlike Washburn capillary flow[30,31] or even Marangoni flow for two-component mixtures without additives, where the different solvent vapor pressures create an interfacial tension gradient,[32] our system requires an emulsion. With mixing, an ensemble of interfaces is produced from the size distribution of droplets that constitute the emulsion.[8] Thus, we make the hypothesis that such a droplet size distribution leads to a spatial gradient of surfactant concentrations, and ultimately a spatial gradient of interfacial tensions is produced. However, we have not employed a precision means to emulsify in these experiments and thus do not have control or knowledge of the droplet size distribution at emulsion formation with hand mixing or magnetic stirring. In addition, mixing of the vial contents to produce an emulsion simultaneously wets the interior glass surface; prewetting of the interior surface is a condition clearly noted by Sastry.[9] Even though we do not separate the mixing and prewetting processes in these experiments, it appears that wetting of the glass surface is necessary to observe the film coat the glass. Hence, the vial material is likely critical to these experiments.

Nanoparticles Are Uniformly Dispersed in the Transferred Film. In our 2005 paper, we experienced difficulty, as have others,[10] in obtaining direct characterization of our film formed at the organic−aqueous interface. We employed a new method in this study, as displayed in Figure 1. Figure 1 displays a representative TEM image of a rather large area of the film, clearly showing the homogeneous dispersal of nanoparticles. Though not crystalline or polycrystalline,[10] uniform coverage is achieved. The inset at right is a second TEM image of the same film, collected at higher resolution. The left inset is a digital photograph of a vial that contains the two phases with film displaced to the glass surface, covering nearly the entire interior of the exposed glass surface. We suggest that Marangoni effects may be exploited to coat surfaces with dispersed or patterned nanostructures in the way that both Pileni and coworkers[33] and recently Cai and Newby realized.[34]

Rate of Film Transfer Depends on Water Fraction and MUA Concentration in the Aqueous Phase. Figure 2 visually displays the dependence of film front distance on the MUA surfactant concentration as well as the fraction of water in the water/ethanol aqueous phase. Vials are allowed to rest for about 5 min following mixing by hand for about 10 s. After 5 min elapsed, an increased mass transfer from the fluid−fluid interface to the glass surface occurs with 10 mM MUA over 5 mM MUA. Additionally, within both MUA concentration series, increased

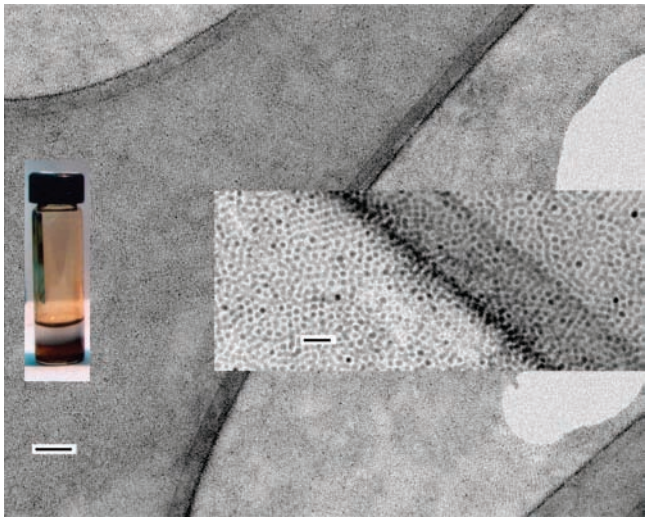

Figure 1. Representative example of displaced film originally formed at the organic−aqueous fluid−fluid interface (60/40 (v/v) water/ethanol, 10 mM MUA in the aqueous phase). Scale bar of main transmission electron microscopy (TEM) image represents 100 nm. Inset at left: a digital photograph of an ordinary, glass laboratory vial, 6 cm in height, with transferred film (80/20 (v/v) water/ethanol and 10 mM MUA in aqueous phase or top layer). Inset at right, center: a higher resolution TEM image of the same film, scale bar represents 20 nm.

mass transfer rates occur with increasing volume fraction of water in the aqueous phase.

Effective Desorption Rate Constant Measured. Effective desorption rate constants were measured for 80/20 (v/v) water/ethanol with 10 mM MUA in the aqueous phase in 1:1 aqueous to chloroform or 2:1 aqueous to chloroform by volume. Charts 1 and 2 show examples of the relative film front distance versus time data recorded for 1:1 and 2:1 aqueous to chloroform by volume, respectively. These data are representative of some of the slowest film transfer rates that we measured for 80/20 (v/v) water/ethanol with 10 mM MUA in the aqueous phase. Chart 1 includes a least-squares fit to $x(t) \sim \exp(-k_{des}t,)$ as provided by eq 10, where k_{des} is the effective desorption rate constant, and yields a fit with $k_{des} = 0.017 \pm 0.001$ s^{-1} (one standard deviation). The first distance, time measurement ($t = 0.00$ s) was not included in the fit. A movie clip of one of the experiments displayed in Chart 1 is provided in Supporting Information. Note the "tears of wine" effect[35] due, in part, to convection of the water/ethanol mixture.[35,36] Chart 2 displays a least-squares fit for the 2:1 aqueous to chloroform by volume data and yields an effective desorption rate constant k_{des} of 0.014 $\pm$ 0.001 s^{-1} (one standard deviation). These effective desorption rate constants are within 2 standard deviations of each other. Moreover, after the 2:1 aqueous to chloroform by volume trials were mixed, some of the emulsion appeared on top of the aqueous layer, as occurred with the 1:1 experiments. However, with the 2:1 experiments, any emulsion *between the fluid layers* quickly separated from the top of the aqueous layer before the beginning of our measurements. Thus, we are confident that any trials where emulsion at the fluid−fluid interface remained connected to the top of the aqueous layer for the 1:1 experiments did not affect the functional form of the $x(t)$ vs time data and did not greatly affect the magnitude of k_{des}.

Our main finding is that this multicomponent system leads to a uniform coating of glass with metallic nanoparticles governed by flow kinetics that are *effectively consistent* with single surfactant desorption kinetics. We initially focused on the 80/20 (v/v) water/ethanol with 10 mM MUA in the aqueous phase experiments because data acquisition was facile. Right away we noticed that even though the climbing film rate pattern

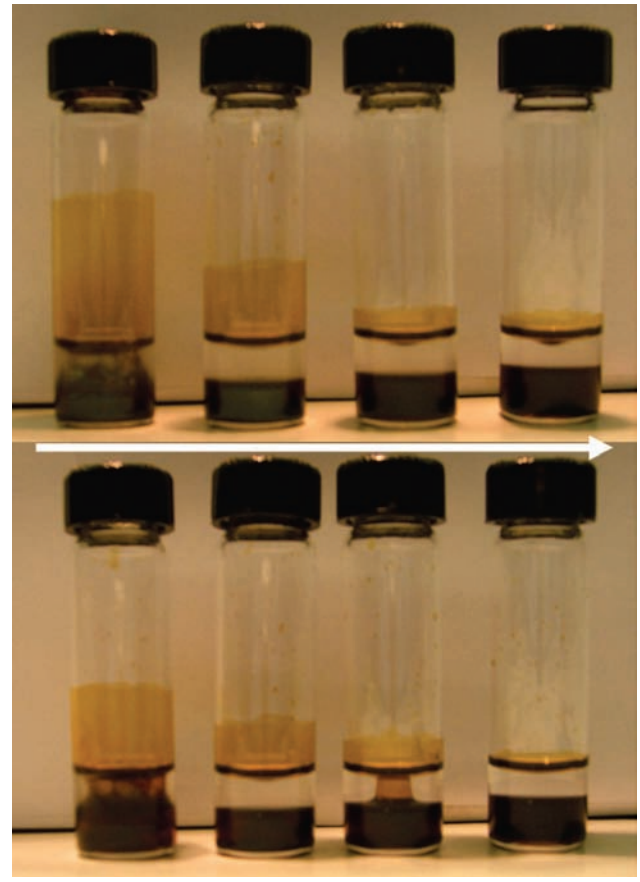

Figure 2. Effect of changing the volume fractions of water and ethanol (v/v) in the aqueous phase (top liquid layer in each vial). Water fraction in aqueous phase decreases from left to right in both top and bottom panels as 80/20, 70/30, 60/40, and 50/50 (v/v) water/ethanol, respectively. After emulsion creation (10 s, mixing by hand) at essentially the same point in time, vials are rested on laboratory bench for 5 min. Digital photographs display 10 mM MUA in aqueous phase (top panel) and 5 mM MUA (bottom panel), respectively. Scale: glass laboratory vials are 6 cm in height. The image in the bottom panel was resized in Photoshop such that the vial height was the same as in the image in the top panel.

CHART 1: Relative Film Front Distance Traveled versus Time for Two Experiments with 80/20 (v/v) Water/Ethanol and 10 mM MUA in the Aqueous Phase and 1:1 Aqueous to Chloroform Volume Proportions[a]

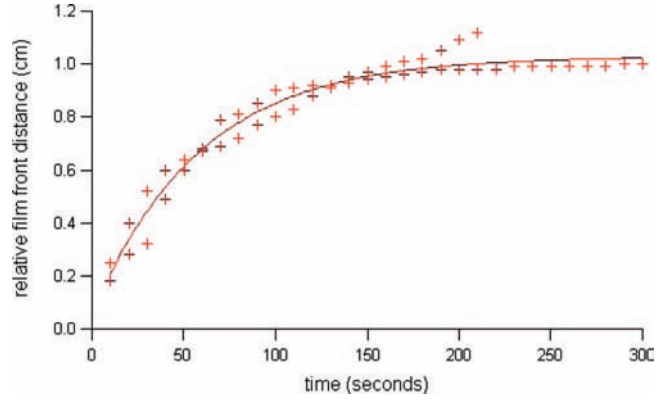

[a] A least squares fit to the functional form of eq 10 yields a $k_{des} = 0.017 \pm 0.001$ s^{-1} to one standard deviation. The uncertainties for the data are ± 0.07 cm and ± 0.1 s, respectively.

CHART 2: Relative Film Front Distance Traveled versus Time for Two Experiments with 80/20 (v/v) Water/Ethanol and 10 mM MUA in the Aqueous Phase for 2:1 Aqueous to Chloroform Volume Proportions[a]

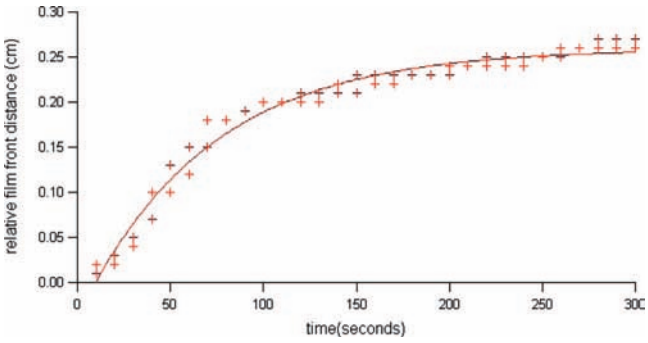

[a] A least squares fit to the functional form of eq 10 yields a $k_{des} = 0.014 \pm 0.001$ s^{-1} to one standard deviation. The uncertainties for the data are ± 0.07 cm and ± 0.1 s, respectively.

($x(t)$ vs time) was reproducible, the fitted k_{des} varied over roughly 2 orders of magnitude (0.01−1 s^{-1}) and its magnitude was affected by how long or by what means the vial was mixed. All in all, over various Ag nanoparticle syntheses, different means of emulsification, and different aqueous to chloroform volume proportions, the data always show an identical climbing rate pattern. However, because of the hypothesized variation of interfacial tension gradients created with mixing, a range for the effective desorption rate constant is reported and we did not make $x(t)$ vs time measurements for other water/ethanol fractions or for 5 mM MUA in the aqueous phase. The effective desorption rate constant is in the range of 0.014−0.55 s^{-1} (data not shown) for 80/20 (v/v) water/ethanol and 10 mM MUA for both 1:1 and 2:1 aqueous to chloroform volume proportions.

Marangoni Flow Rates. Sastry[9] reported 8 cm traveled in about 5 s in a Au colloidal system. Our fastest recorded average rate is about 1 cm in 6 s (a crude average $u = \Delta x/\Delta t$), a measurement that is slower than Sastry's but not inconsistent with his work given the different experimental systems and conditions. In addition, the rate for Marangoni flow for our Ag colloidal system is in accord with that described by Abbott et al.[23] and Cazabat et al.[32] at ∼0.1 cm/s. Notably, the systems of Sastry and ours are quite different from the reversible, electrochemically induced surfactant flow by Abbott and co-workers and the two-component solvent mixture by Fanton and Cazabat, although each system is governed exclusively or mainly by interfacial tension gradients.

Proposed Mechanisms for Flow. Placement of the nanoparticle at the interface provides the opportunity for chemical change. As the film is created, the area of the aqueous fluid/organic fluid contact area is replaced by a nanoparticle, which is wetted at the interface by both aqueous and organic phases. The MUA may adsorb to the nanoparticle surface, or dynamically exchange ligands (with TAB and dodecanethiol) at the nanoparticle surface to change the nanoparticle wettability for assembly at the interface. From prior work on nanoparticle assembly at liquid−liquid interfaces[7] it is known that because of the nanometer size of the particles, the interfacial energy is on the order of kT. Thus, nanoparticle surfactants are dynamic and there can be movement in and out of the interface. The scale of this movement would increase with a decrease in mean nanoparticle size. Additionally, if the nanoparticle wettability is altered by chemisorption or physisorption, the particle will move in and out of the interfacial region due to the change in contact angle (although Young's equation is defined for thermodynamic equilibrium).[37]

Moreover, the emulsion employed to initiate this process is composed of various sized droplets, and as one larger drop divides or two smaller ones coalesce, surfactant will be heterogeneously distributed at the interface.[24] Interfacial areas of comparatively higher surfactant concentration and lower interfacial tension and vice versa are formed. To add to the complexity of our system, all three solvents will evaporate changing interfacial gradients and perhaps local temperatures. In such a scenario, interfacial tension gradients are present and surfactants will flow until a uniform distribution of surfactants is achieved. Thus, the inhomogeneities of MUA and nanoparticle surfactants at the interface following emulsification, with a range of droplet sizes (and hence surface area to volume ratios) are sufficient alone to create the interfacial tension gradients needed to set the interface in motion directed *along the interface*. These dynamical prospects in our experimental system, a self-amplifying[38] or synergistic system, contribute to interfacial turbulence *that simultaneously forms and drives the interface*.

But what causes the film to climb the glass surface? Although our experimental system cannot be assigned solely to a solutocapillary effect, we have shown that MUA surfactant concentration and volume fraction of water in the aqueous phase both affect flow. We suggest that the three phase contact line, where emulsion, vapor, and the prewetted glass surface meet presents another region of interfacial tension gradients. As recently described by Cai and Newby for their system of 100 nm polystyrene particles suspended in ethanol, nanoparticles flow from lower surface tension in the bulk toward a higher surface tension located where the receding contact line and condensed water meet.[34] Our results are consistent with theirs in that large interfacial gradients are created due to solvents and surfactants at the three phase contact line. In addition, we suspect that the borosilicate glass surface properties are critical to observing this film transfer phenomenon although other vial materials were not tested. In sum, the nanoparticle film is entrained in this flow and wets the glass until equilibrium is achieved.

As the film forms, sets into motion and climbs the glass surface, the bulk MUA and nanoparticles may serve to backfill newly opened interfacial areas as the film desorbs to the glass, creating new film area and interfacial tension gradients. If true, subsequent adsorption of surfactant occurs at the recovered aqueous/organic contact area after the nanoparticle flows to the glass. We wondered if adsorption kinetics would be a factor in our film transfer; perhaps adsorption kinetics is important at longer times or with much lower concentrations of surfactant in the bulk. Regardless, these processes in concert cause gradients in a variety of interfacial tensions that both set the interface in motion, and lead to film flow from the fluid−fluid interface to glass until uniform surfactant concentration and thermodynamic equilibrium are achieved. In short, increases in tangential, Marangoni stresses will overwhelm the viscous stresses and energize motion of the interface.

Conclusions

A controlled method to spontaneously coat glass with uniformly distributed Ag nanoparticles has been presented. Our investigation suggests that this flow is governed by creation of interfacial tension gradients within an emulsion and sets the interface in motion according to the Marangoni effect. The Navier−Stokes equation for continuum fluid flow provides a velocity field, and a characteristic velocity scale can be related

to the interfacial tension gradient. This interfacial tension gradient, in turn, is related to the time-dependent surfactant excess at the fluid−fluid interface. A fit of the relative film front distance versus time data yields an effective desorption rate constant for film transfer from the fluid−fluid interface to the glass surface. Our results and analysis show that the nonequilibrium emulsion containing nanoparticles and surfactants contribute to large interfacial tension gradients. We suggest that the use of Marangoni flow may be a profitable means of transferring assemblies formed at the liquid−liquid interface to a solid surface, and we hope that this work may inspire new, creative work in this area.

Acknowledgment. E.M.S. expresses her sincere gratitude to Professor Stephen R. Leone for providing world-class scientific training and outstanding mentorship during and long after her work in his laboratories concluded. In addition, we thank the Camille and Henry Dreyfus Foundation, Inc., the National Science Foundation, the Undergraduate Research Center at Occidental College, the Sherman-Fairchild Foundation, and the Howard Hughes Medical Institute for generous support of this research. We thank Dr. Carol Garland, California Institute of Technology, for her expertise with TEM. We thank Dr. H. Mike Gray, Occidental College, for discussions concerning the Navier−Stokes equation. Finally, we are grateful to Dr. Nathan F. Dalleska, California Institute of Technology, for insightful discussions and editorial comments regarding this manuscript.

Supporting Information Available: An mpeg file with video showing an experiment from Chart 1. The video was clipped to 4:00 min and then compressed for ease of viewing to 1:58 min. This information is available free of charge via the Internet at http://pubs.acs.org.

References and Notes

(1) Shikhmurzaev, Y. D. *Capillary Flows with Forming Interfaces*; Chapman & Hall/CRC: Boca Raton, FL, 2008.
(2) Sternling, C. V.; Scriven, L. E. *AIChE J.* **1959**, *5*, 514.
(3) Squires, T. M.; Quake, S. R. *Rev. Mod. Phys.* **2005**, *77*, 977, and references therein.
(4) Binder, W. H. *Angew. Chem., Int. Ed.* **2005**, *44*, 5172, and references therein.
(5) Binks, B. P.; Horozov, T. S. *Colloidal Particles at Liquid Interfaces*; Binks, Horozov, Eds.; 2006; Cambridge University Press: Cambridge, United Kingdom, Chapter 1, pp 1−74.
(6) Bresme, F.; Oettel, M. *J. Phys.: Condens. Matter* **2007**, *19*, 413101.
(7) Lin, Y.; Skaff, H.; Emrick, T.; Dinsmore, A. D.; Russell, T. P. *Science* **2003**, *299*, 226. Kutuzov, S.; He, J.; Tangirala, R.; Emrick, T.; Russell, T. P.; Böker, A. *Phys. Chem. Chem. Phys.* **2007**, *9*, 6351. Lin, Y.; Böker, H.; Skaff Cookson, D.; Dinsmore, A. D.; Emrick, T.; Russell, T. P. *Langmuir* **2005**, *21*, 191. Russell, J. T.; Lin, Y.; Böker, A.; Su, L.; Carl, P.; Zettl, H.; He, J.; Sill, K.; Tangirala, R.; Emrick, T.; Littrell, K.; Thiyagarajan, P.; Cookson, D.; Fery, A.; Wang, Q.; Russell, T. P. *Angew. Chem., Int. Ed.* **2005**, *44*, 2420.
(8) Dryfe, R. A. W. *Phys. Chem. Chem. Phys.* **2006**, *8*, 1869.
(9) Mayya, K. S.; Sastry, M. *Langmuir* **1999**, *15*, 1902. Kumar, A.; Mandal, S.; Mathew, S. P.; Selvakannan, P. R.; Mandale, A. B.; Chaudhari, R. V.; Sastry, M. *Langmuir* **2002**, *18*, 6478.
(10) Li, Y.-J.; Huang, W.-J.; Sun, S.-G. *Angew. Chem., Int. Ed.* **2006**, *45*, 2537.
(11) Reincke, F.; Hickey, S. G.; Kegel, W. K.; Vanmaekelbergh, D. *Angew. Chem., Int. Ed.* **2004**, *43*, 458. Reincke, F.; Kegel, W. K.; Zhang, H.; Nolte, M.; Wang, D.; Vanmaekelbergh, D.; Möhwald, H. *Phys. Chem. Chem. Phys.* **2006**, *8*, 3828.
(12) Duan, H.; Wang, D.; Kurth, D. G.; Möhwald, H. *Angew. Chem., Int. Ed.* **2004**, *43*, 5639.
(13) Sakata, J. K.; Dwoskin, A. D.; Vigorita, J. L.; Spain, E. M. *J. Phys. Chem. B* **2005**, *109*, 138.
(14) Wang, J.; Wang, D.; Sobal, N. S.; Giersig, M.; Jiang, M.; Möhwald, H. *Angew. Chem., Int. Ed.* **2006**, *45*, 7963.
(15) Park, Y. K.; Yoo, S. H.; Park, S. *Langmuir* **2007**, *23*, 10505.
(16) Lee, K. Y.; Kim, M.; Kwon, S. S.; Han, S. W. *Mater. Lett.* **2006**, *60*, 1622. Lee, K. Y.; Kim, M.; Hahn, J.; Suh, J. S.; Lee, I.; Kim, K.; Han, S. W. *Langmuir* **2006**, *22*, 1817.
(17) Zhang, H.; Edwards, E. W.; Wang, D.; Möhwald, H. *Phys. Chem. Chem. Phys.* **2006**, *8*, 3288.
(18) Murphy, C. J.; Gole, A. M.; Hunyade, S. E.; Stone, J. W.; Sisco, P. N.; Alkilany, A.; Kinard, B. E.; Hankins, P. *Chem. Commun.* **2008**, *5*, 544.
(19) Willets, K. A.; Van Duyne, R. P. *Annu. Rev. Phys. Chem.* **2007**, *58*, 267.
(20) Marangoni, C. G. M. *Ann. Phys. (Poggendorf)* **1871**, *143*, 337. Marangoni, C. *Ann. Phys. Chem.* **1871**, *219* (7), 337.
(21) Bain, C. D. *ChemPhysChem* **2001**, *2*, 580.
(22) McQuarrie, D. A. *Statistical Mechanics*; Harper & Row: New York, 1976.
(23) Bennett, D. E.; Gallardo, B. S.; Abbott, N. L. *J. Am. Chem. Soc.* **1996**, *118*, 6499. Bai, G.; Abbott, N. L.; Graham, M. D. *Langmuir* **2002**, *18*, 9882. Bai, G.; Graham, M. D.; Abbott, N. L. *Langmuir* **2005**, *21*, 2235.
(24) Butt, H.-J.; Graf, K.; Kappl, M. *Physics and Chemistry at Interfaces*; Wiley-VCH: Weinheim, 2003.
(25) Ravera, F.; Ferrari, M.; Liggieri, L. *Adv. Colloid Interface Sci.* **2000**, *88*, 129.
(26) Kovalchuk, N. M.; Vollhardt, D. *Adv. Colloid Interface Sci.* **2006**, *120*, 1.
(27) Pradad, B. L. V.; Stoeva, S. I.; Sorensen, C. M.; Klabunde, K. J. *Chem. Mater.* **2003**, *15*, 935.
(28) Smalley, J. F.; Chalfant, K.; Feldberg, S. W. *J. Phys. Chem. B.* **1999**, *103*, 1676.
(29) Vigorita, J. L. Characterization of Ag Nanoparticle Films at the Liquid-Liquid Interface; Honor's Thesis; Occidental College: Los Angeles, CA, 2005.
(30) Washburn, E. W. *Phys. Rev.* **1921**, *XVII*, 273.
(31) Warren, P. B. *Phys. Rev. E* **2004**, *69*, 041601.
(32) (a) Fanton, X.; Cazabat, A. M. *Langmuir* **1998**, *14*, 2554. (b) Fournier, J. B.; Cazabat, A. M. *Europhys. Lett.* **1992**, *20*, 517.
(33) Maillard, M.; Motte, L.; Ngo, A. T.; Pileni, M. P. *J. Phys. Chem. B* **2000**, *104*, 11871.
(34) Cia, Y.; Newby, B.-M. Z. *J. Am. Chem. Soc.* **2008**, *130*, 6076.
(35) Vuilleumier, R.; Ego, V.; Neltner, L.; Cazabat, A. M. *Langmuir* **1995**, *11*, 4117.
(36) Walters, D. A. *Langmuir* **1990**, *6*, 991.
(37) de Gennes, P. G. *Rev. Mod. Phys.* **1985**, *57*, 828.
(38) Irvin, B. R. *Langmuir* **1986**, *2*, 79.

JP802273J